Indian Journal of Chemistry
Vol. 60A, December 2021, pp. 1564-1573

DFT, TD-DFT and biological activity studies of some maleanilic acid derivatives ligands and their organometallic complexes

Khloud R Oraby[a], Fatma S M Hassan[a], M A Zayed[b], Adila E Mohamed[a] & Islam M Abdellah[a,*]

[a]Chemistry Department, Faculty of Science, Aswan University, Aswan, 81528, Egypt

[b]Chemistry Department, Faculty of Science, Cairo University, Giza, 12613, Egypt

*E-mail: islamabdellah2@aswu.edu.eg

Received 21 September 2021; revised and accepted 26 October 2021

This study is a complementary study to our previous study that included the synthesis and characterization of some maleanilic acid derivative ligands (**L**$^{1-4}$) and their metal carbonyl complexes (**2-4**)**a-d** as effective compounds for cancer cell growth inhibition against three cancer cell lines: HCT-116, HepG-2 cells and MCF-7. The activity data has manifested that the *p*-nitrophenyl maleanilic acid ligand (**L**^{2}) and its chromium complex **(2b)** inhibited the tested cancer cells more effectively than the other complexes. Additionally, DFT and TD-DFT studies are performed to investigate their frontier molecular orbital (FMO), optical properties, and the correlation between the structure and biological activity. The calculated optical energy gap (E_g) is in the range of 1.78- 2.13 eV, and electron cloud delocalization of HOMO/LUMO levels revealed that all complexes show effective charge separation. The DFT results show a strong relation between E_g values of the carbonyl complexes and their experimental biological activity, where it is obvious that complex (**2b**) with the lowest E_g value has the greatest inhibitory potency against cancer cells. In contrast, complex (**2d**) with the highest E_g value exhibits the lowest inhibition potency. These findings translate the inverse relationship between E_g values of the complexes and the inhibition potency against cancer cells.

Keywords: Maleanilic acid derivatives, Organometallic complexes, Anticancer activity, DFT, HOMO/LUMO, TD-DFT

In organometallic chemistry, the fabrication of new complexes plays a significant role in the evolution of organometallic complexes by obtaining unique properties and novel reactivity. Several major aspects must be taken in consideration on studying these metal complexes, such as: the active sites together with the functional groups of ligands, both the behaviour and the properties of the acceptor/ donor atoms of ligands, and the position of the ligand in the coordination sphere of a compound[1-10]. Transition metal carbonyl complexes have more attention in the last decades because of their role in luminescence and electron transfer reactions. Several of these complexes were observed as effective catalysts in catalytic reactions[11] and in pharmacology as antioxidant, coenzyme and anticancer[11-17]. Moreover, in organometallic chemistry metal carbonyl complexes also act as starting materials for other complexes, because the CO ligands can be easily replaced in chemical or photochemical reactions[18]. The chemistry and reactivity of maleanilic acid derivatives have always been of great interest because of their biological activities. They can be used to prepare maleimides, which act as chemical probes of protein structure[19], and they can also be used as preventative and curative fungicides[20]. Maleanilic acid derivatives play an important role in polymer chemistry because they can be used as photo initiators in free-radical polymerization[21,22]. They can also be used as monomers in polymaleimides or their copolymers synthesis. Maleimides find further application in the agricultural industry as herbicides and fungicides[23]. Furthermore, aryl-substituted of maleimides have been synthesized for use as new acetylcholinesterase inhibitors, which are being researched for the treatment of Alzheimer's disease[24]. On the other hand, the computational chemistry[25] is rapidly growing which involves the use of home computers for the interpretation of experimental results[26].

In our previous work, we have synthesized some maleanilic acid derivatives as bidentate free ligands (*p*-methoxy phenyl, *p*-nitrophenyl, *p*-chloro phenyl and *p*-fluoro phenyl maleanilic acid). The prepared free ligands have chelated with the chromium group hexacarbonyls to give organometallic complexes of the formula [R(C_6H_4) NHCOCH=CH-COOH-M $(CO)_4$]; in which (M = Cr, Mo, W) and (R= OCH_3, NO_2, Cl or F). All the free ligands and their

complexes were characterized using elemental analyses, mass spectrometry, FT-IR, ^{1}H-NMR spectroscopy and thermal analyses[27-29]. In this study we mainly focused on studying the cytotoxic activity of the prepared maleanilic acid derivatives and their carbonyl complexes against three cancer cell lines in comparison with the theoretical calculations to confirm their life importance as health applications. Furthermore, DFT and TD-DFT studies were performed to obtain more information on HOMO/LUMO energy levels and to investigate the relationship between the energy gap (E_g) values of the complexes and the inhibition efficacy against cancer cells.

Materials and Methods

All the chemicals needed for this study were purchased from Sigma Aldrich (Germany) and Alpha Aesar. Those chemicals included $Cr(CO)_6$, $Mo(CO)_6$, $W(CO)_6$, maleic anhydride, 4-methoxyaniline, 4-nitroaniline, 4-chloroaniline, 4-fluoroaniline, DMF, DMSO and absolute ethanol solvent.

Synthesis of the free ligands and their metal carbonyl complexes

The maleanilic acid derivatives **(L^{1-4})** were prepared according to the procedures reported in the literature[30] as shown in Scheme 1. Maleic anhydride 9.8 g (0. 1 mol) and aniline derivatives **(1a-d)** (0.1 mol) were mixed and ground at room temperature in an agate mortar. The grinding was continued for 30-60 min. The crude products were crystallized from ethanol several times and the collected crystals were dried. On the other hand, the metal carbonyl complexes **(2-4)a-d** were prepared according to the procedures reported in the literatures[27-29] as shown in Scheme 1 by dissolving the free maleanilic acid derivatives ligands **(L^{1-4})** (0.5 mmol) in a few amount of DMF and then $M(CO)_6$ (0.5 mmol) in the same solvent was added. The total volume was made to 20 mL with the same solvent. The obtained reaction mixture was stirred for 40-60 min at 90-100 ºC under reflux in an inert nitrogen atmosphere. The product was separated and washed thoroughly with ethanol several times and recrystallized from DMF / ethanol mixture. Finally the product was dried by means of P_2O_5 in a desiccator. All the free ligands and their complexes was confirmed by different spectral techniques such as FT-IR, ^{1}H-NMR, elemental analysis, mass spectroscopy, and thermal analysis (see Supplementary Data, Tables S1-S3 & Figs. S1–S52).

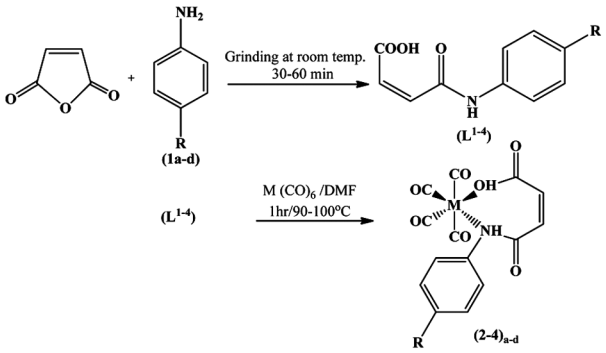

Scheme 1 — Synthesis of N-substituted maleanilic acid ligands **(L^{1-4})** and metal carbonyl complexes **(2-4)a-d**, where: R=OCH_3 (**L^1**); R=NO_2 (**L^2**); R= Cl (**L^3**); R=F (**L^4**). M=Cr, R=OCH_3 (**2a**); M=Cr, R=NO_2 (**2b**); M=Cr, R= Cl (**2c**); M=Cr, R=F (**2d**); M=Mo, R=OCH_3 (**3a**); M= Mo, R=NO_2 (**3b**); M= Mo, R= Cl (**3c**); M= Mo, R=F (**3d**); M=W, R=OCH_3 (**4a**); M= W, R=NO_2 (**4b**); M= W, R= Cl (**4c**); M= W, R=F (**4d**)

Cell culture and cytotoxicity determination

Three human cancer cell lines; HCT-116 (colon cancer), HepG-2 cells (human hepatocellular cancer) and MCF-7 (human breast cancer) were obtained frozen in liquid nitrogen (-180 ℃) for in vitro screening experiments from Tissue Culture Unit (VACSERA). Serial sub-culturing was used to keep the tumor cell lines alive at the National Cancer Institute in Cairo, Egypt. Cell culture cytotoxicity assays were carried out as described previously[18]. DMEM medium was used for culturing and maintenance of the human tumor cell lines[18].

The cells were grown in DMEM and supplemented with 10% heat-inactivated fetal bovine serum, 1% L-glutamine, HEPES buffer and 50 µg mL^{-1} gentamycin. All of the cells were kept at 37 ℃ in a humidified atmosphere with 5% CO_2, and then subcultured twice a week. The cells were seeded in 96-well plate at a cell concentration of 1×10^4 cells / well in 100 µL of growth medium. After that, a fresh medium with different concentrations of the tested sample was added after one day of seeding. A multichannel pipette was used to add serial two-fold dilutions of the investigated chemical compound to confluent cell mono layers dispensed into bottomed micro titer plates (Falcon, NJ, USA). The micro titer plates were incubated at 37 ℃ in a humidified incubator with 5% carbon dioxide for two days. Three wells were used for each concentration of the tested sample. Control cells were incubated without test sample and with / without DMSO. After cells incubation at 37 °C, various concentrations of sample were added and the incubation was continued for 24 h

and viable cells yield was determined by the colorimetric method [31].

Molecular modeling

Equilibrium molecular geometries of **(2-4)a-d** complexes were calculated using density functional theory (DFT) utilizing Becke 3-Parameter (Exchange), Lee, Yang and Parr (correlation) (B3LYP) exchange correlation function and SDD function basis set. Also, the vertical excitation energy and their response (UV–visible absorption) in the excited complexes were computed using TD-DFT calculations at CAM-B3LYP/SDD. All DFT and TD-DFT calculations were carried out using Gaussian 09 program package[32].

Results and Discussion

Biological activity

The cytotoxic activity of chromium carbonyl chelates of the type [R(C_6H_4) NHCOCH=CH-COOH-Cr$(CO)_4$]; which R = (NO_2, Cl or F) and the corresponding ligands against cell lines of HCT-116, hepG-2 and MCF-7 was evaluated by viability assay. The concentrations of them ranged from 3.9 µg mL^{-1} to 500 µg mL^{-1}, the inhibitory percentage against growth of cancer cells was determined. The IC_{50} values obtained for ligands and their chelates against selected three tumor cell lines are shown in Table 1, the toxicity of the ligands and chelates was found to be concentration dependent, the cell viability decreased with increasing the concentration of them against the tested cancer cell lines. The biological activities of $\mathbf{L^{2-4}}$ free ligands and their chromium complexes are presented in Figs. S53-S69, Supplementary Data.

Cytotoxic activity of the free ligands

Cytotoxicity *in vitro* of *p*-nitrophenyl maleanilic acid free ligand $\mathbf{L^2}$ has been estimated by MTT assay against three typical human tumor cell lines involving HepG-2, MCF-7 and HCT-116. The results are presented in Fig. 1a. The results of inhibitory rate of *p*-nitrophenyl maleanilic acid free ligand show remarkable cytotoxicity (IC_{50}) against the selected human cancer cell lines in the following order: HepG-2 (15.1µg mL^{-1}) > MCF-7 (25.9 µg mL^{-1}) > HCT-116 (26.7 µg mL^{-1}). While, *p*-chlorophenyl maleanilic acid free ligand $\mathbf{L^3}$ introduced lower inhibitory activity against the three selected human tumor cell lines as shown in Fig. 1b, compared to the inhibitory activity of *p*-nitrophenyl maleanilic acid $\mathbf{L^2}$. This is due to the lower electronegativity of chloro-group in $\mathbf{L^3}$ compared to that of nitro group in $\mathbf{L^2}$. Moreover, the results of inhibitory rate of *p*-nitrophenyl maleanilic acid free ligand showed a higher cytotoxicity against the selected human cancer cell

Table 1 — Influence of the compounds on the viability of MCF-7, HepG-2 and HCT-116 cell lines

Compound	In vitro cytotoxicity IC_{50} (µg mL^{-1})		
	HepG-2	MCF-7	HCT-116
$\mathbf{L^2}$	15.1	25.9	26.7
$\mathbf{L^3}$	123	95.2	60.4
$\mathbf{L^4}$	60.4	56.2	53.7
2b	27.3	30.1	29.6
2c	91.2	163	236
2d	>500	>500	>500

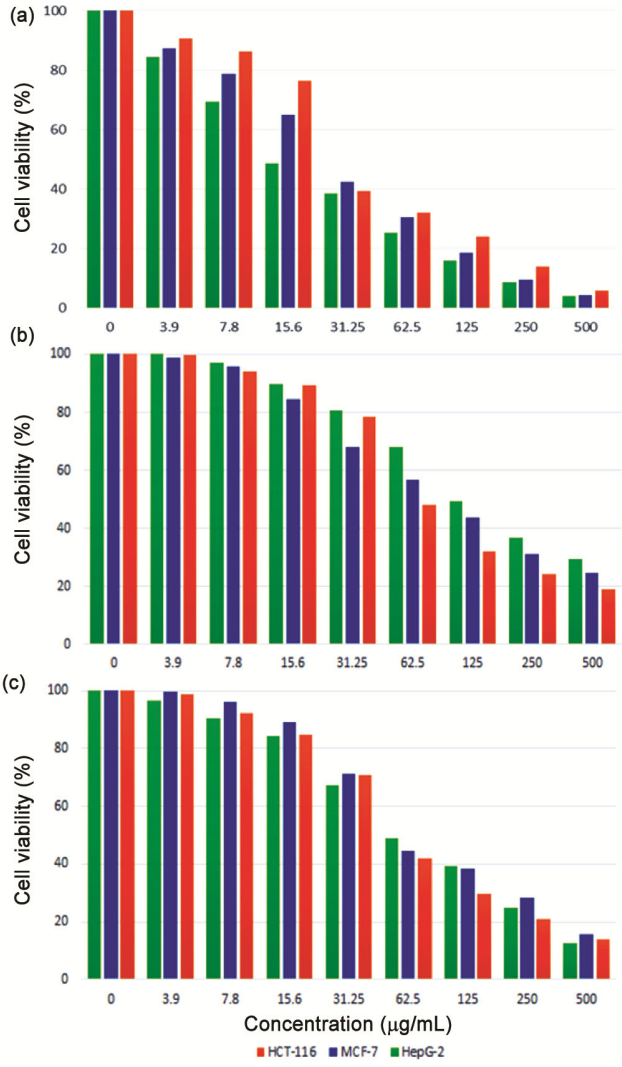

Fig. 1 — Cell viability of ligands (a) $\mathbf{L^2}$, (b) $\mathbf{L^3}$ and (c) $\mathbf{L^4}$, against the three tested cell lines

lines compared to that of $\mathbf{L^2}$ and has the following order: HCT-116, (60.4 µg mL^{-1}) > MCF-7 (95.2 µg mL^{-1}) > HepG-2 (123 µg mL^{-1}). Furthermore, evaluation of the efficacy of *p*-fluorophenyl maleanilic acid free ligand $\mathbf{L^4}$ as inhibitor revealed a higher potency against HepG-2, MCF-7and HCT-116 human cancer cell lines, compared to that of *p*-chlorophenyl maleanilic acid free ligand $\mathbf{L^3}$ as shown in Fig. 1c. This is attributed to the replacement of the less electronegative 4-chlorophenyl moiety of *p*-chlorophenyl maleanilic acid free ligand $\mathbf{L^3}$ with the more electronegative 4-fluorophenyl moiety of *p*-fluorophenyl maleanilic acid free ligand resulted in enhancement of the inhibitory activity. The calculated IC_{50} of $\mathbf{L^4}$ showed lower values than that of $\mathbf{L^3}$ and have the following order: HCT-116 (53.7 µg mL^{-1}) > MCF-7 (56.2 µg mL^{-1}) > HepG-2, (60.4 µg mL^{-1}) as shown in Table 1. Finally, the cytotoxic activity of the free ligands $\mathbf{L^{2-4}}$ was found to be in the order $\mathbf{L^2 > L^4 > L^3}$ depending on the electronegativity of the para position substituents in the free ligand.

Cytotoxic activity of metal complexes

The cytotoxic activity of all chelates of the type of $[R(C_6H_4)NHCOCH{=}CH\text{-}COOH\text{-}Cr(CO)_4]$; where, R = ($NO_2$, Cl or F) against cell lines of HCT-116, HepG-2 and MCF-7 was evaluated by viability assay. The cell viability (%) obtained with continuous exposure for 24 h at different concentrations ranging from (0-500 µg mL^{-1}) is depicted in Fig. 2. Treatment of the cell lines with $[O_2N(C_6H_4)\ NHCOCH{=}CH\text{-}COOH\text{-}Cr\ (CO)_4]$ leads to significant decrease in the cell viability of the tested cell lines with increasing the concentration of it, as shown in Fig. 2a. The IC_{50} values are 27.3, 30.1 and 29.6 µg mL^{-1} for HepG-2, MCF-7 and HCT-116 cell lines, respectively, these values of IC_{50} of $[O_2N(C_6H_4)\ NHCOCH{=}CH\text{-}COOH\text{-}Cr\ (CO)_4]$ complex are slightly less than that of $\mathbf{L^2}$ free ligand, as shown in Table 1. The cytotoxic activity of $[Cl(C_6H_4)NHCOCH{=}CH\text{-}COOH\text{-}Cr\ (CO)_4]$ against cell lines of HepG-2, MCF-7 and HCT-116 was evaluated and depicted in Fig. 2b. The IC_{50} values are 91.2, 163 and 236 µg mL^{-1} for HepG-2, MCF-7 and HCT-116 cell lines, respectively, Table 1. The calculated IC_{50} values of $[Cl(C_6H_4)\ NHCOCH{=}CH\text{-}COOH\text{-}Cr(CO)_4]$ illustrated that the $[Cl(C_6H_4)NHCOCH{=}CH\text{-}COOH\text{-}Cr(CO)_4]$ demonstrated lower inhibitory activity against the tested cell lines comparing to the corresponding $\mathbf{L^3}$ free ligand except for HepG-2 cell line, the $[Cl(C_6H_4)NHCOCH{=}CH\text{-}COOH\text{-}Cr(CO)_4]$ has higher inhibitory activity than the $\mathbf{L^3}$ free ligand. The cytotoxic activity of $[F(C_6H_4)NHCOCH{=}CH\text{-}COOH\text{-}Cr(CO)_4]$ was assayed and depicted in Fig. 2c. The IC_{50} values were estimated from the respective dose response curve and are summarized in Table 1. The resulted data obtained from the cytotoxic activity assay of $[F(C_6H_4)NHCOCH{=}CH\text{-}COOH\text{-}Cr\ (CO)_4]$ illustrated that the inhibitory potency of the $\mathbf{L^4}$ free ligand was obviously weakened when complexed with $Cr(CO)_6$. In conclusion, the free ligands ($\mathbf{L^{2-4}}$) outperformed the corresponding chromium complexes **(2b-c)** in terms of inhibitory potency against the tested cell lines.

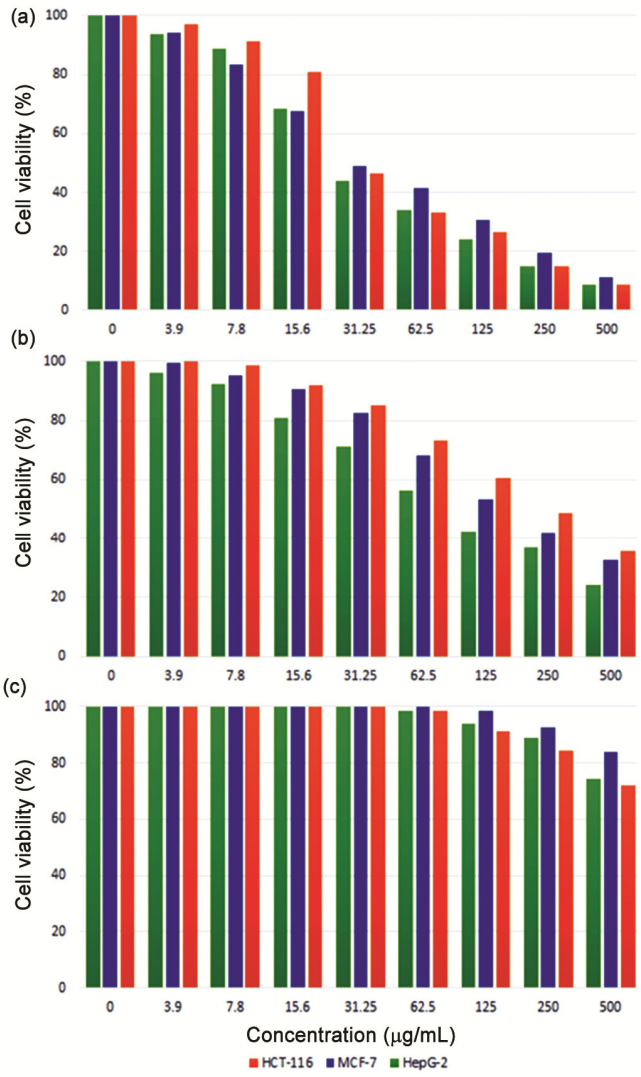

Fig. 2 — Cell viability of complexes (a) **2a**, (b) **2c** and (c) **2c,** against the three tested cell lines

The comparison of the inhibitory activity of p-nitrophenyl maleanilic acid (**L**^{2}), p-chlorophenyl maleanilic acid (**L**^{3}), and p-fluorophenyl maleanilic acid (**L**^{4}) derivative ligands against the detected cell lines result in, *p*-nitro maleanilic acid and exhibits the highly inhibitory activity against the three selected human tumor cell lines. The IC_{50} values are 15.1 µg mL^{-1}, 25.9 µg mL^{-1} and 26.7 µg mL^{-1} for HepG-2, MCF-7 and HCT-116, respectively. **L**^{4} has the second potency with IC50 values of 56.2, 60.4 and 53.7 µg mL^{-1} for HepG-2, MCF-7 and HCT-116 human cancer cell lines, respectively, while, **L**^{3} has the least potential for all the selected cell lines. The high activity of **L**^{2} may be assigned to the high electronegativity of nitro substituent of the ligand followed by **L**^{4} of high electronegativity and the small size, then **L**^{3} ligand is cleared the least activity one because it has less electronegativity. On the other hand, among the chromium chelates **(2b-c)**, the *p*-nitrophenyl maleanilic acid chromium carbonyl chelate **(2b)** exhibits the highest inhibition potency against the tested cell lines, whereas, the chromium chelate of *p*-fluorophenyl maleanilic acid **(2d)** exhibits the least inhibitory activity. It was obvious that, the potency of the *p*-chlorophenyl maleanilic acid ligand with chromium metal **(2c)** against HepG-2 cell lines has been improved compared to the free ligand (**L**^{3}).

Molecular modeling of (2-4) a-d complexes

The quantum estimations are viewed as one of the most dependable computational methodologies in the field of chemistry. The DFT calculations were done for complexes **(2-4)a-d** at B3LYP energy functional and basis set (SDD) utilizing Gaussian 09 software. The Fermi Molecular Orbitals (FMO) of the complexes indicates the effective charge separation in HOMO-LUMO energy levels as depicted in Table 2. As expected, in their HOMO orbitals, the electron cloud is predominantly more accumulated on the donor part of complexes **(2-4)a-d** which includes the metal (Cr, Mo, W) and the carbonyl groups with come electron density on the aromatic ring. While, the LUMO levels for complexes **(2-4)a-d** the electron cloud is shifted evidently from the electron donor to the electron acceptor which represents the metal (Cr, Mo, W) and the synthesized ligands (**L**$^{1-4}$), but in different extent depends up on the nature of the substituted groups (P-OCH_3, NO_2, F, Cl) on the ligand molecules.

DFT calculations were performed to evaluate the HOMO LUMO levels and the optical energy gap (E_g) as shown in Table 3. The optical energy gap (E_g) was calculated using the formula $E_g = E_{HOMO} - E_{LUMO}$. From the E_g values it was observed that there is a great relation between the E_g values and the nature of the substituted groups such as (OCH_3, NO_2, Cl, F) on the ligand molecules. The E_g values of all complexes were found to be of the following order F > Cl > OCH_3 > NO_2. Moreover, the nature of metals (Cr, Mo, W) play a vital role in the E_g values which follow the order of Cr > Mo > W, as observed in Fig. 3. These E_g values were reflected in the light absorption characteristics of the molecules which showed the tungsten based complexes (E_g= 1.78-1.79 eV) absorbs light radiation in a wider range compared to the chromium (E_g= 2.11-2.13 eV) and molybdenum (E_g= 1.96-1.98 eV) based complexes. In conclusion, theoretically, the donating properties of the studied complexes as indicated from the computed E_{HOMO} follow the order of the following substituent OCH_3 > Cl > F > NO_2. Meanwhile, they can be arranged according to the metals to have the following order W > Mo > Cr.

TD-DFT for complexes **(2-4)a-d** have been performed to check their lowest singlet-singlet electronic excitation energy ($E_{0\text{-}0}$) and UV-visible absorption spectra and the findings are summarized in Table 4 and Fig. 4. The TD-DFT was performed on the optimized structure at CAM-B3LYP & SSD basis set and the solvent effect was neglected. It was evident from the TD-DFT measurements that the calculated absorption spectra of the complexes showed two regions of bands in the range 310–395 nm due to π–π* electronic transitions and the other bands in the range 505–570 nm, which could be due to metal-to-ligand charge transfer as for the chromium complex (Cr, $d_{\pi\text{-}\pi^*}$) or due to ligand-to-metal charge transfer as for molybdenum and tungsten complexes (π*-M, dπ)[33] From the results, it was obvious that ligand-to-metal charge transfer of tungsten complexes **(4a-d)** are bathochromic shifted by an average of $\Delta\lambda_{max}$=60 nm corresponding to molybdenum complexes **(3a-d)** and an average of $\Delta\lambda_{max}$=47 nm corresponding to metal-to-ligand charge transfer of chromium complexes **(2a-d)**. The maximum electronic absorption spectra can be arranged according to the metals size to have the following order W > Mo > Cr. Thus, in the case of tungsten complexes **(4a-d)**, it would show significant

Table 2 — Fermi molecular orbitals for complexes **(2-4)a-d**

Complex	Optimized Structure	HOMO	LUMO
2a	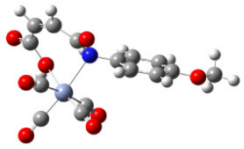	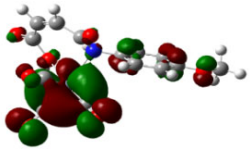	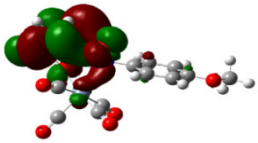
2b	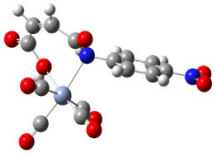	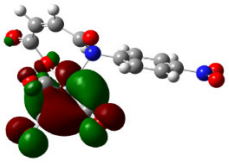	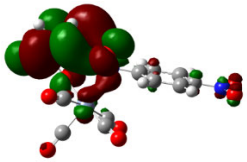
2c	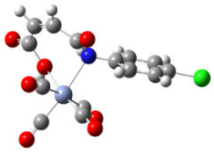	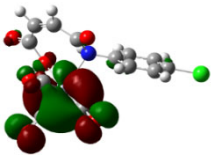	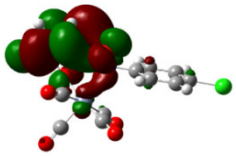
2d	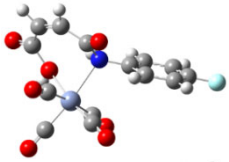	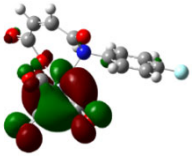	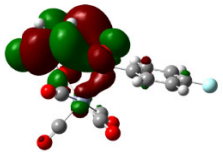
3a	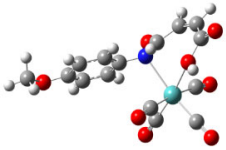	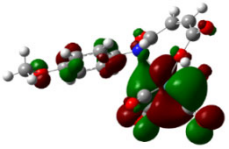	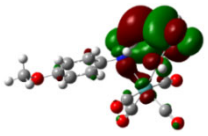
3b	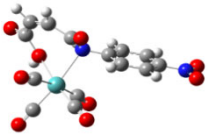	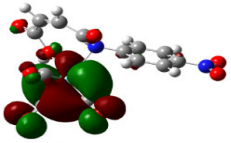	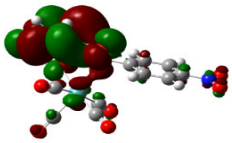
3c	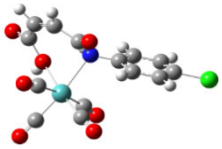	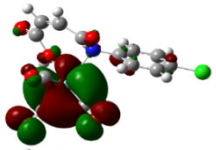	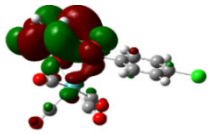
3d	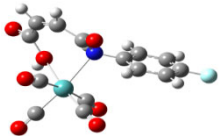	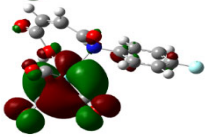	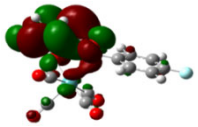
4a		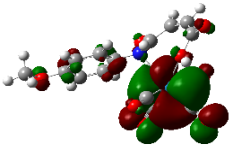	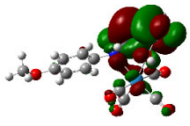
4b	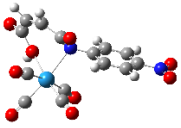	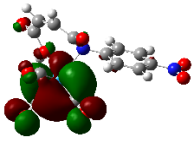	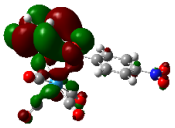

(contd.)

Table 2 — Fermi molecular orbitals for complexes **(2-4)a-d** *(contd.)*

Complex	Optimized Structure	HOMO	LUMO
4c	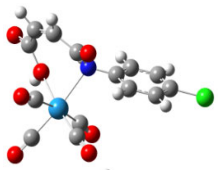	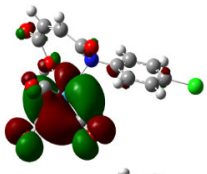	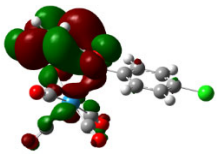
4d	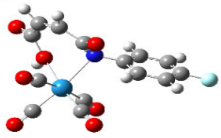	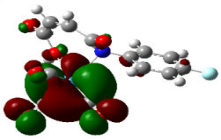	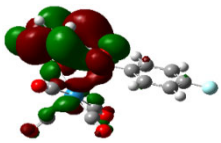

Table 3 — HOMO, LUMO, the optical energy gap (E_g) and dipole moment (μ) values for complexes **(2-4)a-d** computed by B3LYP and SSD basis set

Complex	E_{HOMO} (hartree)	E_{HOMO} (eV)	E_{LUMO} (hartree)	E_{LUMO} (eV)	E_g (eV)	μ (D)
2a	-0.22431	-6.103788	-0.14611	-3.97585	2.12793	8.5700
2b	-0.23970	-6.522571	-0.16205	-4.40960	2.11297	8.7159
2c	-0.23157	-6.301342	-0.15321	-4.16905	2.13229	7.2133
2d	-0.23162	-6.302703	-0.15324	-4.16987	2.133653	7.2523
3a	-0.22119	-6.018888	-0.14885	-4.05041	1.968478	9.2082
3b	-0.23649	-6.435223	-0.16440	-4.47355	1.961673	9.1887
3c	-0.22841	-6.215354	-0.15573	-4.23763	1.977724	7.8104
3d	-0.22855	-6.219164	-0.15573	-4.23763	1.981534	7.8477
4a	-0.21762	-5.921744	-0.15217	-4.14075	1.780994	9.6788
4b	-0.23265	-6.330731	-0.16722	-4.55028	1.780451	9.4220
4c	-0.22470	-6.114400	-0.15886	-4.32280	1.7916	8.1949
4d	-0.22492	-6.120387	-0.15887	-4.32307	1.797317	8.2177

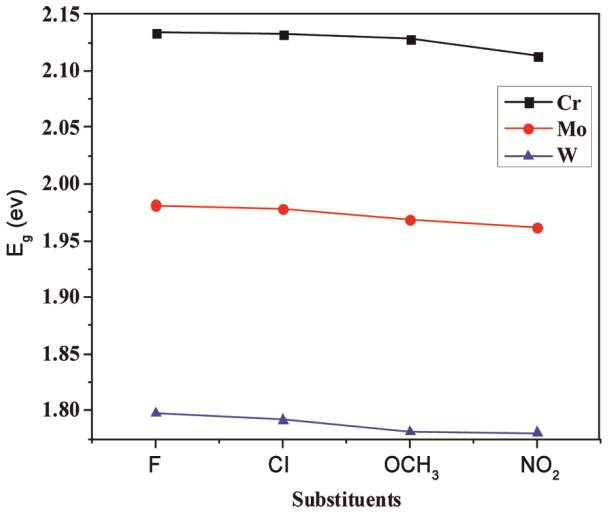

Fig. 3 —Plots for the relation between E_g, the nature of ligands and metals

bathochromic shifts perhaps due to high charge density and consequently strong bonding with the ligand molecule compared to that of chromium **(2a-d)** and molybdenum **(3a-d)** complexes.[34] The absorption spectra of the complexes confirm the effect of changing the metal (M) on the position of the visible absorption of the complexes. On the other hand, Tungsten complexes showed a good maximum molar absorptivity in the range of (2306–2482 M^{-1} cm^{-1}) compared to that of molybdenum (1893–2010 M^{-1} cm^{-1}) and chromium complexes (1415–1338 M^{-1} cm^{-1}). Among all metal complexes, the complexes incorporating nitro substituted ligand achieved the highest molar absorptivity compared to other complexes of the same metal.

The relation between E_g-values of the complexes and biological activity

The comprehensive study of the molecular modelling and the cytotoxicity of the chromium carbonyl complexes of some selected ligands ($\mathbf{L^{2\text{-}4}}$) it was obvious that, there is a great relation between E_g of the carbonyl complexes and their biological activity towards HCT-116, HepG-2 and MCF-7 cells. It is well known that the E_g values have a relative effect on the reactivity of the drugs or complexes under consideration. The greater the energy gap, the lower the corresponding hardness values, implying

Table 4 — Maximum absorption wavelength (λ), Molar absorptivity (ε), oscillator strength (*f*) and the first excitation energy ($E_{0\text{-}0}$), values for complexes **(2-4)a-d** computed at CAM-B3LYP and SSD basis set

Metal	Complex	λ (nm)	ε ($M^{-1}cm^{-1}$)	*f*	$E_{0\text{-}0}$ (eV)
	2a	362 (π–π*)	3856.89	0.0115	2.1587
Cr		520 (π*- dπ)	1338.93		
	2b	358 (π–π*)	1647.78	0.0102	2.1437
		522 (π*- dπ)	1415.78		
	2c	342 (π–π*)	2590.40	0.0103	2.1550
		520 (π*- dπ)	1381.45		
	2d	347 (π–π*)	2232.10	0.0100	2.1554
		518 (π*- dπ)	1362.68		
	3a	384 (π–π*)	2421.88	0.0081	2.134
Mo		505 (π*- dπ)	1893.05		
	3b	313 (π–π*)	1124.37	0.0064	2.110
		514 (π*- dπ)	2010.16		
	3c	322 (π–π*)	2110.46	0.0065	2.127
		509 (π*- dπ)	1985.15		
	3d	320 (π–π*)	1730.16	0.0062	2.130
		509 (π*- dπ)	1977.70		
	4a	394 (π–π*)	1879.19	0.0057	1.869
W		567 (π*- dπ)	2306.45		
	4b	349 (π–π*)	1192.88	0.0047	1.848
		567(π*- dπ)	2482.08		
	4c	324 (π–π*)	1652.83	0.0049	1.863
		567 (π*- dπ)	2444.19		
	4d	321 (π–π*)	1287.38	0.0047	1.866
		564 (π*- dπ)	2440.29		

high reactivity of the investigated complexes[35,36]. This is due to the molecules' increased ability to accept electrons more readily, which will most likely be reflected in their reactivity[36]. It should be noted, however, that while energy gap and hardness parameters correlate with a molecule's chemical reactivity in general, they do not always reflect its biological activity, as the latter is dependent on a variety of other parameters and effects[35]. The molecular modelling results show that, the E_g of the chromium complexes follow the order of **2d** (2.133 eV) > **2c** (2.132 eV) > **2b** (2.112 eV), which is the same order for the decreasing complexes potency towards the cancer cells as **2d** < **2c** < **2b**. This gives an interpretation of the decreasing of the E_g of the metal chelate enhance the potency of it to the cancer cells. In conclusion, the *p*-nitrophenyl maleanilic acid metal carbonyl complex (**2b**) exhibits the highest inhibition potency against the tested cell lines. Meanwhile, the chelation of *p*-chlorophenyl maleanilic acid ligand with chromium metal (**2c**) makes it highly active than the free ligand and the metal complex of *p*-fluorophenyl maleanilic acid exhibits the least inhibitory activity (**2d**). This explains the importance of designing chromium complexes incorporating highly electronegative groups and with lower E_g in order to enhance its efficiency to cancer cells. Furthermore, the TD-DFT study showed a relation between molar absorptivity of the carbonyl complexes and their biological activity towards selected cell lines. Where, the TD-DFT results show that, the molar absorptivity of metal-to-ligand charge transfer (π*-dπ) for chromium complexes follow the order of **2b** (1415.78 M^{-1} cm^{-1}) > **2c** (1381.45 M^{-1} cm^{-1}) > **2d** (1362.68 M^{-1} cm^{-1}), which is the same order for the increasing complexes potency towards the cancer cells as follow **2b** > **2c** > **2d**. This explains the potency of the complex to the cancer cells enhanced by increasing the molar absorptivity of the metal chelate. Moreover, the outstanding molar absorptivity of tungsten complexes **(4a-d)** makes it a promising candidate for cancer cells.

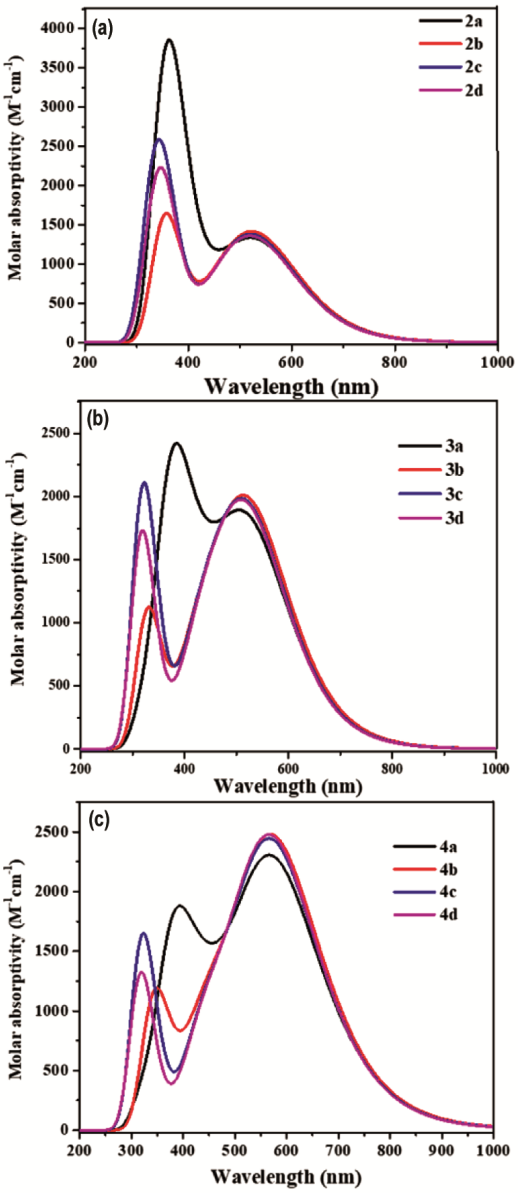

Fig. 4 — Calculated UV-visible absorption spectra of **(2-4)a-d** complexes at CAM-B3LYP/SDD

Conclusions

Four maleanilic acid derivatives incorporating (*p*-methoxy phenyl, *p*-nitrophenyl, *p*-chloro phenyl and *p*-fluoro phenyl maleanilic acid) were used as bidentate free ligands for the synthesis of different metal carbonyl complexes of the formula [R(C_6H_4) NHCOCH=CH-COOH-M$(CO)_4$]. The cytotoxic activity of some selected maleanilic acid ligands incorporating *p*-nitrophenyl, *p*-chloro phenyl, and *p*-fluoro phenyl ($\mathbf{L^{2\text{-}4}}$) have been examined for anticancer activities against HepG-2, MCF-7 and HCT-116 cancer cells and achieved an efficacy in the order of $\mathbf{L^2}$ > $\mathbf{L^4}$ > $\mathbf{L^3}$ depending on the electronegativity of the para position substituents in the ligand. Meanwhile, the cytotoxic activity of their chromium carbonyl complexes **(2b-c)** on the same cancer cells were in the order of **2b>2c>2d**. In general, the overall inhibition potency of the free ligands ($\mathbf{L^{2\text{-}4}}$) against cancer cells outperformed that of the corresponding chromium complexes **(2b-c)**, with the exception of the p-chlorophenyl maleanilic acid ligand with chromium metal (2c) against HepG-2 cell lines, which has been improved over the free ligand ($\mathbf{L^3}$). These results have been confirmed from the comprehensive study of both DFT/TD-DFT and the cytotoxicity of the metal carbonyl complexes **(2-4)a-d**. It was obvious that the complexes incorporating nitro groups e.g. (**2b**) achieved the lowest E_g, the highest molar absorptivity values and shows the highest inhibition potency against the three tested cell lines and vice versa with complexes incorporating fluorine atom e.g. (**2d**) that demonstrated the significant concordance between the E_g of the complexes and their experimental biological activity. In summary, we have recommended the importance of designing chromium complexes from ligands of maleanilic acid derivatives that incorporate high electronegativity groups with low E_g and high molar absorptivity in order to enhance their efficacy on cancer cells.

Supplementary Data

Supplementary Data associated with this article are available in the electronic form at http://nopr.niscair.res.in/jinfo/ijca/IJCA_60A(12)1564-1573_SupplData.pdf.

Acknowledgement

The authors are thankful to Regional Center for Mycology & Biotechnology, Al-Azhar University, Cairo, Egypt, for providing biological activity facilities.

References

1 Amini M M, Najafi E, Babaei M, Ghahramani K & Khavasi H R, *Monatshefte fur Chemie*, 147 (2016) 1547.
2 Bharty M K, Paswan S, Dani R K, Singh N K, Sharma V K, Kharwar R N & Butcher R J, *J Mol Struct*, 1130 (2017) 181.
3 Calu L, Badea M, Chifiriuc M C, Bleotu C, David G I, Ioniță G, Măruțescu L, Lazăr V, Stanică N, Soponaru I, Marinescu D & Olar R, *J Therm Anal Calorim*, 120 (2015) 375.
4 Ledeți I, Vlase G, Vlase T, Bercean V & Fuliaș A, *J Therm Anal Calorim*, 121 (2015) 1049.

5 Lintnerová L, Valentová J, Herich P, Kožíšek J & Devínsky F, *Monatshefte für Chemie - Chem Mon*, 149 (2018) 901.

6 Mandal M, List M, Teasdale I, Redhammer G, Chakraborty D & Monkowius U, *Monatshefte für Chemie - Chem Mon,* 149 (2018) 783.

7 Murthy Y L N, Govindh B, Diwakar B S, Nagalakshmi K & Rao K V R, *Med Chem Res*, 21 (2012) 3104.

8 Najafi E, Amini M. M, Taherbateni S, Memarian H & Ng S W, *Monatshefte für Chemie - Chem Mon*, 149 (2018) 1379.

9 Zayed E M, Zayed M A & El-Desawy M, *Spectrochim Acta A*, 134 (2015) 155.

10 Zhai Q G, Hu M C, Wang Y, Ji W J, Li S N & Jiang Y C, *Inorg Chem Commun*, 12 (2009) 286.

11 Kimmich B F M, Fagan P J, Hauptman E, Marshall W J & Bullock R M, *Organometallics*, 24 (2005) 6220.

12 Bandarra D, Lopes M, Lopes T, Almeida J, Saraiva M S, Vasconcellos-Dias M, Nunes C D, Félix V, Brandão P, Vaz P D, Meireles M & Calhorda M J, *J Inorg Biochem*, 104 (2010) 1171.

13 Datta P, Mukhopadhyay A P, Manna P, Tiekink E R, Sil P C & Sinha C, *J Inorg Biochem*, 105 (2010) 577.

14 Glans L, Taylor D, de Kock C, Smith P J, Haukka M, Moss J R & Nordlander E, *J Inorg Biochem*, 105 (2011) 985.

15 Zhang W-Y, Banerjee S, Hughes G M, Bridgewater H E, Song J-I, Breeze B G, Clarkson G J, Coverdale J P C, Sanchez-Cano C, Ponte F, Sicilia E & Sadler P J, *Chem Sci*, 11 (2020) 5466.

16 Huang H, Banerjee S, Qiu K, Zhang P, Blacque O, Malcomson T, Paterson M J, Clarkson G J, Staniforth M, Stavros V G, Gasser G, Chao H & Sadler P J, *Nat Chem*, 11 (2019) 1041.

17 Huang C, Liang C, Sadhukhan T, Banerjee S, Fan Z, Li T, Zhu Z, Zhang P, Raghavachari K & Huang H, *Angew Chemie Int Ed*, 60 (2021) 9474.

18 Arifin K, Daud W R W & Kassim M B, *Ceram Int*, 39 (2013) 2699.

19 Corrie J E T, *J Chem Soc Perkin Trans* 1 (1994) 2975.

20 Fujinami A, Ozaki T, Nodera K & Tanaka K, *Agr Biol Chem,* 36 (2014) 318.

21 Boyd P D W, Challis J B & Rickard C E F, *Acta Crystallogr Sect E: Struct. Rep. Online*, 62 (2006) m2732.

22 Rich D H, Gesellchen P D, Tong A, Cheung A & Buckner C K, *J Med Chem*, 18 (1975) 1004.

23 Bastin L D, Nigam M, Martinus S, Maloney J E, Benyack L L & Gainer B, *Green Chem Lett Rev*, 12 (2019) 127.

24 Trujillo Ferrara J, Correa Basurto J, Espinosa J, García J, Martínez F & Miranda R, *Synth Commun*, 35 (2006) 2017.

25 Mulholland P & Dundas D, *Phys Rev A*, 97 (2018) 043428.

26 Mura P, Faucci M T, Maestrelli F, Furlanetto S & Pinzauti S, *J Pharm Biomed Anal*, 29 (2002) 1015.

27 Oraby K R, Zayed M A, Hassan F S M & Mohamed A E, *J Transit Met Complexes*, 2020 (2020) 1.

28 Zayed M A, Hassan F S M, Mohamed A E & Oraby K R, *J Transit Met Complexes*, 2018 (2018) 1.

29 Zayed M A, Oraby K R & Hassan F S M, *Egypt J Chem*, 63 (2020) 4327.

30 Saedi H, *Bull Chem Soc Ethiop*, 27 (2013) 137.

31 Mosmann T, *J Immunol Methods*, 65 (1983) 55.

32 Frisch M, Trucks G, Schlegel H, Scuseria G, Robb M, Cheeseman J, Scalmani G, Barone V, Petersson G & Nakatsuji H, Gaussian 16, Gaussian, Inc. Wallingford, CT, (2016).

33 El-Medani S M, *J Coord Chem,* 57 **(**2006) 497.

34 Panhwar Q K & Memon S, *Sci World J*, 2014 (2014) 845208.

35 Piechowska K, Mizerska-Kowalska M, Zdzisińska B, Cytarska J, Baranowska-Łączkowska A, Jaroch K, Łuczykowski K, Płaziński W, Bojko B, Kruszewski S, Misiura K & Łączkowski K. Z, *Int J Mol Sci*, 21 (2020) 1.

36 Mishra A K & Tewari S P, *SN Appl Sci,* 2 (2020) 1.